2026 IEEE International Conference on Robotics and Automation (ICRA 2026)
June 1-5, 2026. Vienna, Austria

Development of a Mixed-control Ankle Assist Device with Sensor-fusion-based Phase Recognition for Walking Exercise Promotion

Chang-Wen Wang, *Student Member, IEEE*, Donglin Wang, *Student Member, IEEE*, Huan Wang, Shuo Yan, Keisuke Osawa, *Member, IEEE*, Kei Nakagawa, and Tanaka Eiichiro, *Member, IEEE*

***Abstract*— "Frail" elderly often experience walking impairments that limit independence and sustained physical activity. Although various assistive devices exist, many rely on single-mode control, limiting adaptability, responsiveness to gait variability, and voluntary motion. To improve, we developed a wearable ankle-assist device with real-time gait phase recognition and multi-mode control. Sensor fusion of inertial and plantar-pressure data enables robust five-phase segmentation, with optimal weights tuned by Particle Swarm Optimization. Based on detected gait phase, the controller dynamically switches between speed, torque, and free modes, adapting to cadence variations. Treadmill experiments showed that mixed control increased walking distance (251 m to 282 m ($p < 0.05$)), reduced heart rate change (20% to 10% ($p < 0.01$)). Gait analysis confirmed comfort and less resistance. These findings demonstrate that phase-aware adaptive assistance balances propulsion and natural motion, supporting mobility and reducing strain. This framework provides a practical basis for wearable ankle-assist systems in elderly rehabilitation and daily use.**

I. Introduction

As global aging accelerates, muscle degeneration and neurological disorders such as stroke have emerged as major contributors to mobility impairment, reducing independence and quality of life in older adults [1]–[3]. Although moderate-intensity physical activity is beneficial for preserving cardiovascular and musculoskeletal function, many elderly individuals struggle to sustain walking exercise because of sarcopenia and diminished joint coordination [4]. On the emotional state, research has been done to encourage them to walk longer, and give stimulation when the user wants to stop [5]–[8]. On the physical state, elderly often have difficulty to keep their toes high enough to prevent collapsing with the ground. There are many exoskeletons used in clinical environment to correct human's motion and prevent this kind of situation [9]–[12]. Although they usually support multiple functions [13], [14], they are too bulky for daily activities. Even with lighter version, a full leg exoskeleton is still not suitable for daily activities [15].

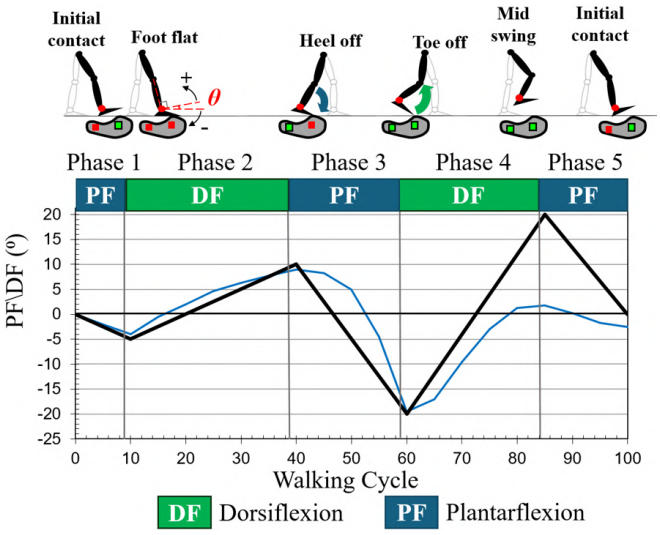

Fig. 1. Diagram of the walking cycle segmented into five distinct gait phases with example linear line.

Advised by the medical doctor, the ankle assistance could exploit the stretch reflex of bi-articular muscles to achieve efficient foot clearance [16], [17]. The human gait cycle is commonly segmented into five phases defined by biomechanical events, as illustrated in Fig. 1. This research mainly focus on supproting the foot kicking and the beginning of foot swinging phase, which one provides the user a forward inertia, and the other one is using dorsiflexion to provide clearance between the foot and the ground. During dorsiflexion assistance, the gastrocnemius (GAS) is stretched and reflexively contracts, inducing knee flexion, followed by rectus femoris (RF) activation driving hip flexion. This sequence of reflexes enables efficient clearance without relying on the tibialis anterior, aligning external actuation with natural biomechanics. A conceptual illustration of this mechanism is shown in Fig. 2. By utilizing this concept, a simple ankle assist device can induce the user to raise their foot higher to prevent from hazards. Further experiments also proved this concept [18].

Chang-Wen Wang is with the Graduate School of Information, Production, and Systems, Waseda University, Fukuoka, 808-0135, Japan(e-mail: changwenwang@toki.waseda.jp).

Donglin Wang is with the Graduate School of Information, Production, and Systems, Waseda University, Fukuoka, 808-0135, Japan(e-mail: donglin-wang@akane.waseda.jp).

Huan Wang was with the Graduate School of Information, Production, and Systems, Waseda University, Fukuoka, 808-0135, Japan(e-mail: wangh19971@asagi.waseda.jp).

Shuo Yan is with the Graduate School of Information, Production, and Systems, Waseda University, Fukuoka, 808-0135, Japan(e-mail: yan@toki.waseda.jp).

Keisuke Osawa is with the Department of Mechanical Engineering, Faculty of Engineering, Kyushu University, Fukuoka, 808-0135, Japan.(e-mail: k-osawa@mech.kyushu-u.ac.jp).

Kei Nakagawa was with the Graduate School of Biomedical and Health Sciences, Hiroshima University, 1-2-3 Kasumi, Minami-ku, Hiroshima 734-8551, Japan.

Eiichiro Tanaka is with the Graduate School of Information, Production, and Systems, Waseda University, Fukuoka, 808-0135, Japan(phone: 093-692-5043; e-mail: tanakae@waseda.jp).

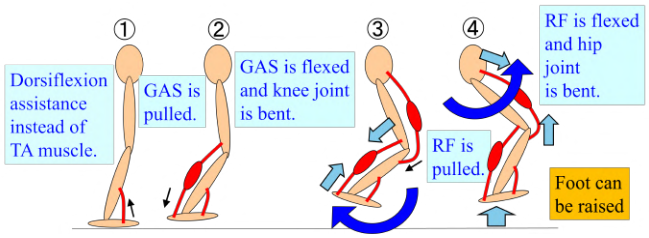

Fig. 2. Conceptual illustration of the reflexive flexion mechanism.

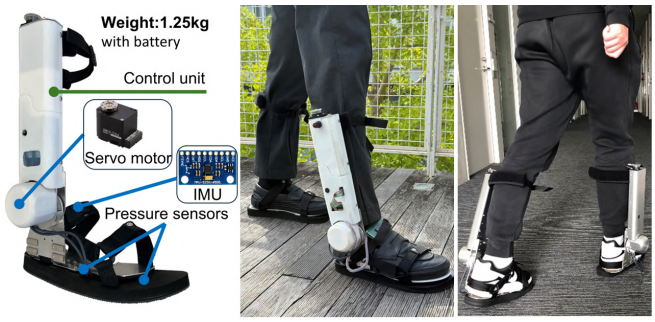

Fig. 3. Ankle-assist device and user wearing condition corresponding to the control strategy illustrated in this study.

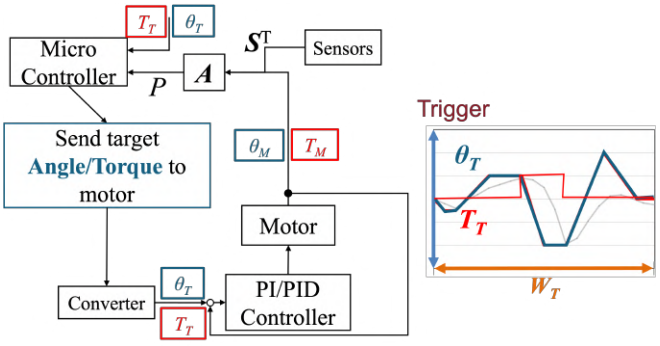

Fig. 4. Real-time control framework from sensor input to motor. Notations: W_T: target walking cycle; W_{TL}: estimated target walking cycle using linear regression; W_{TQ}: estimated target walking cycle using quadratic fitting; θ_T: target ankle angle; θ_M: output angle of motor; T_T: target torque; T_M: output torque of motor; P: calculated value for walking phase recognition; ω: coefficient of each sensor parameter; S: sensor parameters.

Generally, ankle assist device can be divided into two types: passive and active device. Passive devices redistribute biomechanical energy without powered actuation [19]–[22]. They can reduce joint load under specific conditions but lack phase-dependent adaptability, as shown in Chen et al.'s waist-mounted design [23]. Active devices integrate actuators and sensors to provide adaptive support [24], [25], which can reduce the muscle usage and improve user's walking motion [26]–[29]. However, some limitation existed, such as miss estimation of the gait motion, which may cause increasement of muscle usage compared with not wearing the device [30]. Additionally, current exoskeletons are mainly for clinical environment, which is safe and protected. This paper focus on solving these issues and develop a practical ankle assist device suitable for elderly's daily outdoor activities to prevent them from becoming frail.

In this study, an active ankle-assist device is employed as an experimental evaluation platform. The system integrates fused-sensor gait recognition, optimized by Particle Swarm Optimization for robust five-phase detection, with a flexible controller capable of switching among speed, torque, and free modes. Through treadmill trials, the proposed framework is shown to enhance walking efficiency and reduce cardiovascular load compared with conventional single-mode strategies, providing new evidence that adaptive, phase-specific control offers a practical and effective basis for ankle-centered walking assistance.

II. System Design and Control Framework

The device utilized in this research is shown in Fig. 3. It is an ankle assist device using a Kendo PMX-SCR-9203HV motor, with maximum torque of 8.07 Nm and an Arduino Mega2560 as a controller [31], [32]. 2 flexiable pressure sensors are attached on the bottom of the shoe, which can measure upto 2 kg of weight, used to detect whether the user's foot has contact the ground. Toe and heel has one on each, which allows the device to determine the gait phase user is currently in. The control logic is as shown in Fig. 4, in which the sensors are used to detect the user's motion and determine which gait phase the user is currently, allowing the device to provide the suitable assist.

However, user's walking cycle time isn't usually constant, and misalignment of each phase's activation time can cause discomfort or causing the user to lose balance. In order to fit user's walking pattern, the time between heel strike and toe off is measured with the pressure sensor. Then, it is used to estimate the gait cycle time using the method in this research [33], which combined a linear regression and the quadratic fitting to find a suitable gait cycle time for the next step, as Fig. 5 shown. With correct timing being estimated, the adjustment angle can then be determined with the data collected from the real human [33]. To this end, the device can adjust the ankle angle to induce more propelled force for faster walking, and vice versa.

This control system enables dynamic adaptation to cadence variations for synchronized and comfortable assistance. However, gait segmentation and cycle adjustment remain limited, especially only the pressure sensor is introduced at the beginning. Pressure sensors often produced overlapping or unstable signals, failing to reliably distinguish swing sub-phases, as shown in Fig. 6. In contrast, dorsum IMU signals exhibited distinct features corresponding to swinging gait phases: gyroscope peaks highlighted Phases 1 and 5 (Fig. 7), while quaternion components captured Phases 4 and 5 (Fig. 8). Therefore, with the combination of IMUs and pressure sensors, the device can robustly distinguish all five gait phases.

Therefore, seven sensors were decided to install on to the device (three MPU9250 IMUs on the shank, dorsum, and toe; and two pressure sensors) [34]. IMUs are especially added to identify the difference between phase 4 and phase

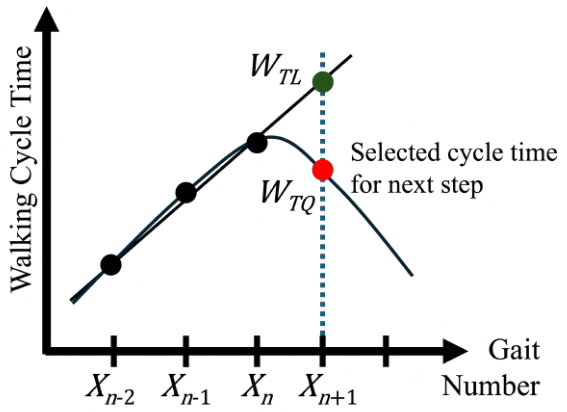

Fig. 5. Estimation of target walking cycle using combination of linear regression and quadratic fitting [33].

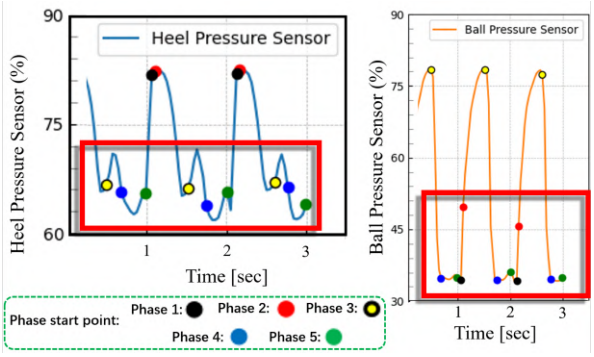

Fig. 6. Results of pressure sensor data, in which shows that the data fluctuated significantly during different gait phases. The left figure is the heel pressure data, and the right figure is the toe pressure data. The pressure data is not able to distinguish the pre-swing and swing phase.

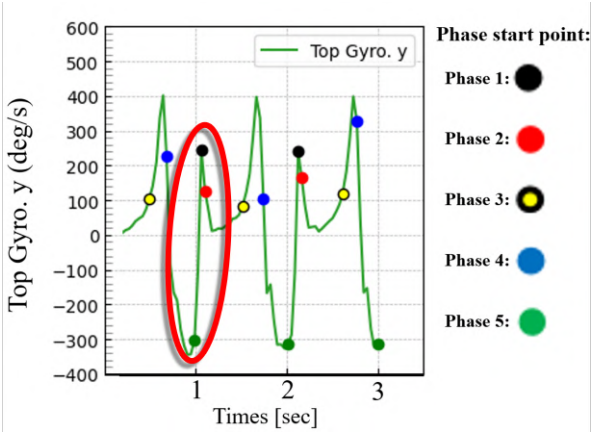

Fig. 7. Dorsum IMU gyroscope y-axis peaks corresponding to gait Phases 1 and 5.

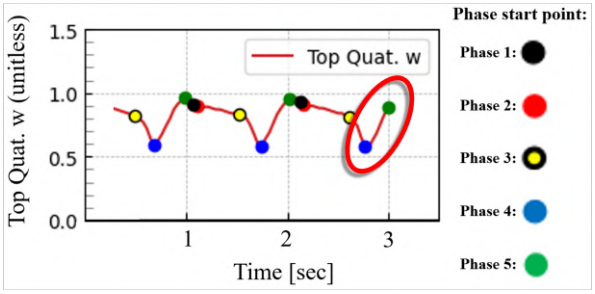

Fig. 8. Dorsum IMU quaternion components and signals highlighting gait Phases 4 and 5.

5, which is directly effecting the user's safety as mentioned in 1. Additionally, we noticed that the device is not providing enough torque in the toe off phase in practical use.

To address these issues, this research proposed a method to (i) fuse different sensor data for phase determination, (ii) use partical swam optimization method to let the machine to learn from collected dataset, and (iii) discuss about the difference when mixing different control method in different phase.

III. Sensor Fusion Based Phase Detection

A. Phase Recognition with Fused Sensors

As established in the previous section, neither plantar-pressure sensors nor inertial measurement units (IMUs) alone can robustly identify all five gait phases due to inherent limitations. To address this, the fusion model is proposed to combine the strengths of both sensor modalities. It is modeled as a linear combination of n normalized sensor signals, with feature vector $S(t) = [s_1(t), \ldots, s_n(t)]^T$ and coefficient vector $\omega = [\omega_1, \ldots, \omega_n]^T$. The model is defined as Eq. 1, where $s_i(t)$ denotes the normalized sensor input at time t, and ω_i is the weighting coefficient that determines its contribution.

The expected output $P(t)$ is a continuous scalar function that can be discretized into integer labels from 1 to 5, each representing the timing of Heel Strike, Foot Flat, Heel Off, Toe Off, and Mid Swing. IMU-derived accelerations and angular velocities capture limb dynamics, quaternion components encode foot orientation, and plantar pressure signals describe ground contact. Together, these features form a continuous representation of gait evolution over time.

$$P(t) = \sum_{i=1}^{n} \omega_i \cdot s_i(t) \tag{1}$$

B. PSO-Based Coefficient Optimization

Although the linear formulation of the P-value is straightforward, the parameter space is high-dimensional and the mapping between sensor signals and gait phases is nonlinear. Manual selection of coefficients is therefore impractical, motivating the use of Particle Swarm Optimization (PSO) [35] to automatically identify the weight set that maximizes recognition accuracy. The optimization criterion is defined as

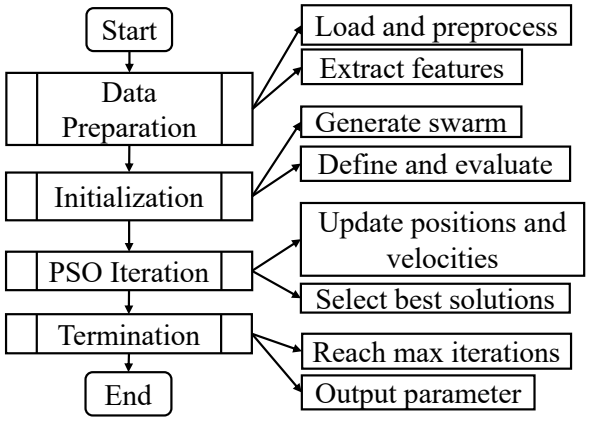

Fig. 9. Flowchart of the PSO Algorithm for Weight Optimization.

Eq. 2, where $N_{correct}$ is the number of correctly recognized phases using coefficients w, and N_{total} is the total number of labeled samples. By minimizing $J(w)$, PSO converges to an optimized coefficient vector that balances IMU, orientation, and plantar pressure contributions. Training was performed using synchronized IMU and plantar-pressure data with motion-capture labels as ground truth.

$$J(\omega) = 1 - \frac{N_{\text{correct}}(\omega)}{N_{\text{total}}} \tag{2}$$

The training process is as illustrated in Fig. 9. After raw sensor signals are collected from the device, they are preprocessed to reduce noise on the dataset. For preprocessing, IMU angular velocities is collected directly from the MPU9250's digital motion processing (DMP), which already provided with low-passed, stablized quaternion data. Then, the angular velocities were high-pass filtered to remove the long-term drift, using a cutoff frequency of 0.1 Hz. Later, the filtered signals were substituted into the model function with PSO-optimized coefficients to do phase estimation. Then, the estimation is compared against the ground truth labels to get the error, which is used for optimization. This training process allows us to find the most robust coefficients for the model to robustly estimate five gait phases across both stance and swing.

With the correct model being found by the PSO optimization, stable recognition of all five gait phases is achieved. Leveraging this capability, this method is integrated in to the controller in Fig. 4. During walking, IMU and pressure sensors capture motion and form a normalized feature vector s, which is weighted by the optimized coefficient vector ω and processed by the microcontroller. The controller computes the recognition score P and, once hysteresis and dwell-time conditions are met, triggers updated control targets—walking cycle W_T, the ankle angle trajectory θ_T, or the target torque T_T—that are transmitted through a converter to the actuator.

IV. Hybrid Assist for Walking Phases

The assist strategy for each phase still remains to be defined. Previous studies utilized only speed control, resulting in limited supportiveness on human motion. As a result, a hybrid control strategy is proposed, in which torque, speed, or no output control (free mode) is applied depending on the gait phase, as illustrated in Fig. 10. The condition we focused the most in this research is phase 3, which provides the user a forward inertia for stable walking. Therefore, the torque control is applied in this phase, while other phases remain using speed control. Additionally, we tested the effect of free mode in phase 1 and phase 5, which are providing the user a margin to adjust their gait pattern according to the environment, which is expected to reduce the mechanical resistance and improve the comfort.

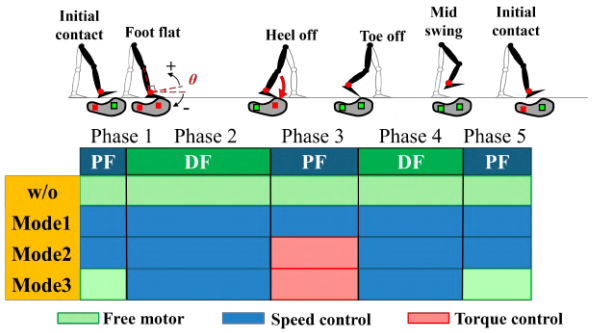

Fig. 10. Control strategy schematic showing four assistive modes across five gait phases.

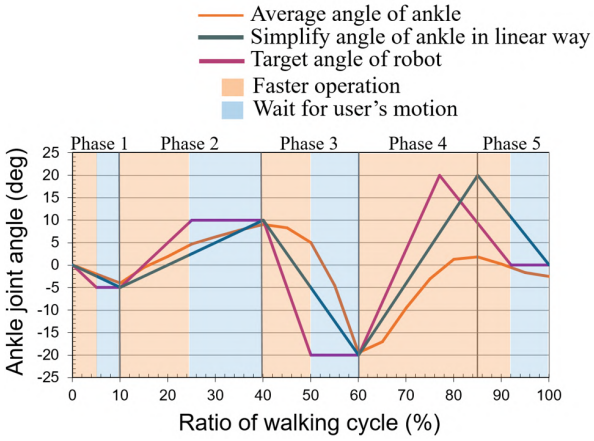

Fig. 11. An example promoting method of ankle assist device.

Different feedback controllers are used depending on the motor outputting method: a PID loop regulates ankle angle θ when the speed control method is utilized, while a PI loop regulates torque T for torque control method. A gait-phase scheduler is implemented to determine the control angle or torque that is required in the current timing of the gait cycle, including switching between different controllers and adjust the target value. The half timing concept is utilized to ensure the device is always one step ahead of the user, as shown in Fig. 11, where the motor is always moving slightly faster than the user, and wait for the next phase to start [33].

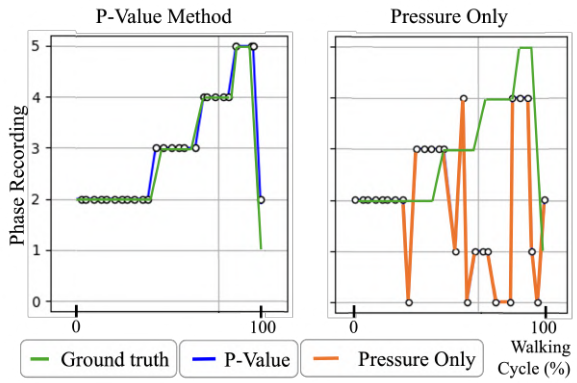

Fig. 12. Phase judgement in one cycle. P-value with reduced sensors, stably recognizing all five phases, while Pressure-only method, showing misclassifications and zero outputs.

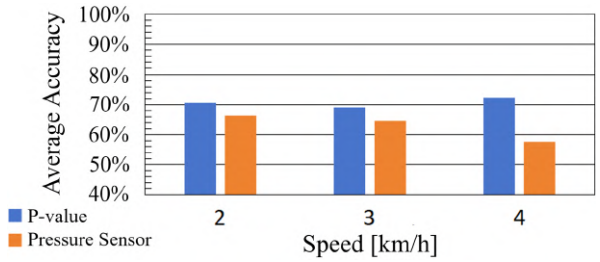

Fig. 13. Average phase recognition accuracy of all participants.

V. Experiment and Discussion

A. Phase Estimation

To evaluate the proposed P-value method, treadmill experiments were conducted with six healthy male participants (age 23-26 years, height 167-177 cm, weight 62-73 kg) to evaluate the accuracy of the proposed method. Participants are asked to walk at different speeds (2, 3, and 4 km/h), and all signals were synchronously recorded at 100 Hz using the ankle-assist device. The sensor readings have been collected and analyzed beforehand, in which we discovered only using two IMUs (shank, dorsum) and two pressure sensors (toe, heel) shows significance in practical applications. Therefore, these sensor values are used during the experiment Additionally, the video is recording the user's motion on the treadmill, which is used to determine the ground truth of gait phases using Tracker [36].

Recognition accuracy was quantified against a reference trajectory using Eq. 3, where $n_{correct}$ is the number of correctly identified phases and n_{all} is the total number of samples. This metric reflects the proportion of accurate classifications, with higher values indicating better performance.

$$\text{Accuracy} = \left(\frac{n_{\text{correct}}}{n_{\text{all}}} \right) \times 100\% \tag{3}$$

The training results are shown in Fig. 12, in which the one using the proposed method is on the left, and the original pressure sensor phase determination method is on the right. The proposed method is more accurate than the original method. Additionally, it remains more stable in recognizing the gait phase compared with the pressure-only method, which the latter frequently misclassifies phases that may cancel out the output from the device.

On the statistical side, accuracy mostly improved from 57.48% with pressure sensors to 70.61% with the P-value method at 4 km/h, as shown in Fig. 13. This demonstrates the coefficients trained using PSO were transferred effectively to simplified hardware and confirm the robustness of the fusion approach.

This presented experiment confirmed that PSO-optimized coefficients generalized well, showing better estimation of gait phases on different walking speeds on different participants. It is considered as a promising method to improve the accuracy of gait phase recognition, due to the fact that human walking pattern is not fixed and varies between 2-4 km/h, and it is able to improve the general recognition accuracy. Together, these results demonstrate that the proposed method provides a robust and practical foundation for phase-specific control in the ankle-assist device.

B. Mixed Control Evaluation

To evaluate the impact of different assistive control strategies on gait performance and physiological effort, treadmill experiments were conducted with walking distance and heart rate change as the primary outcomes. Greater distance within the fixed trial duration was interpreted as enhanced mobility, while smaller heart rate increases reflected reduced physiological load. Six healthy adult volunteers without gait or cardiovascular disorders participated.

The ankle-assist device was applied bilaterally using standardized fastening protocols to ensure consistent fit. Each subject completed four trials: three under distinct control modes and one unassisted baseline. Trial order was randomized to minimize sequence effects, and participants were blinded to the active mode. Each trial consisted of 15 minutes of treadmill walking at a comfortable, self-selected pace, followed by a 10-minute seated rest for recovery.

Gait and physiological data were sampled at the 2nd and 14th minutes of each trial to capture temporal changes. Stride length, cadence, and heart rate were extracted as outcome measures, with gait data analyzed using Kinovea software [37] and heart rate continuously recorded with an Apple Watch [38]. Relative heart rate change was calculated to quantify physiological effort across assistive modes.

To compare the three assistive control strategies, key biomechanical and physiological indicators were analyzed from the walking trials. The group-level outcomes included total walking distance, relative change in heart rate, and proportional changes in stride length and cadence between the 2nd and 14th minutes. These parameters capture both the physiological demands and gait adaptations under different control conditions. Walking distance was computed according to Eq. 4.

$$D = \frac{C \times S \times \text{Time}}{2} \tag{4}$$

where D is walking distance [m], S is stride length [m], C is cadence [step/min] and Time [min]. This formulation reflects the product of step frequency, average stride length, and total walking duration, yielding a consistent estimate of locomotor output across conditions.

Statistical analysis employed the Wilcoxon signed-rank test for pairwise comparisons and the Friedman test for repeated measures [39], [40], with significant differences annotated in the plots. Heart rate change, stride length change rate, and cadence change rate were all derived using the relative change formula in Eq. 5, where x represents the measured variable at the specified timepoints—namely, heart rate, stride length, or cadence, CR is the change rate.

$$CR = \frac{x_{\text{end}} - x_{\text{start}}}{x_{\text{start}}} \times 100\% \tag{5}$$

The experimental outcomes highlight four key findings on how control strategies affect physiological load and gait dynamics. Heart rate change, cadence, stride length, and walking distance were analyzed across six participants. Modes 1-3 correspond to full-phase speed, torque-plus-speed, and torque-plus-free strategies, while w/o indicates walking without assistance. Error bars denote standard error (SE), and *, **, and *** indicate $p < 0.05$, $p < 0.01$, and $p < 0.001$, respectively.

Average walking distance increased from 251 m in the w/o condition to 282 m in Mode 3 ($p < 0.05$), but dropped to 225 m in Mode 1 ($p < 0.01$) (Fig. 14). Heart rate change decreased from 20% (w/o) to 10% in Mode 3 ($p < 0.01$) (Fig. 15). For cadence and stride length, all three modes with w/o show the trend of increasing in Figs. 16-17. Since cadence and stride length varied differently across participants—some increasing and others decreasing—we further calculated their ratios to enable fair comparison, as illustrated in Fig. 18, both Mode 1 and Mode 2 showed reductions compared with w/o, whereas Mode 3 improved stride length and reduced cadence. Together, these results underscore the dual benefit of Mode 3, improving both biomechanical output and physiological efficiency.

To visualize relative improvements, Figs. 19 show the ratios of walking distance and heart rate change between mode combinations. Each ratio is computed by dividing the value of one mode by another (e.g., w/o:m1 is the distance in Mode 1 divided by that in w/o). In Fig. 19a, w/o:w/o serves as the baseline, significant differences were observed in comparisons between w/o:w/o and w/o:m1 (**), w/o:w/o and w/o:m3 (*), w/o:m1 and w/o:m2 (***), w/o:m1 and w/o:m3 (***), and w/o:m2 and w/o:m3 (*). For heart rate change (Fig. 19b), significant differences were found between w/o:w/o and w/o:m2 (*), w/o:w/o and w/o:m3 (**), w/o:m1 and w/o:m3 (***), and w/o:m2 and w/o:m3 (*). SE bars are shown, and w/o to m3 follow the mode definitions above. These results confirm that mixed-control strategies, especially Mode 3, improve gait performance and reduce physiological load compared with baseline.

Regarding the CR of cadence and stride length, both Mode 1 and Mode 2 showed minimal improvement com-

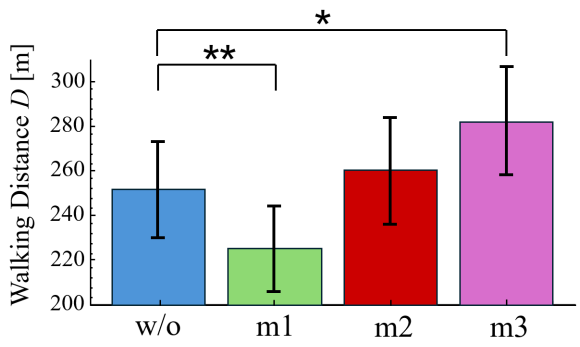

Fig. 14. Average walking distance in 15 minutes across different modes under user's own comforting walking speed.

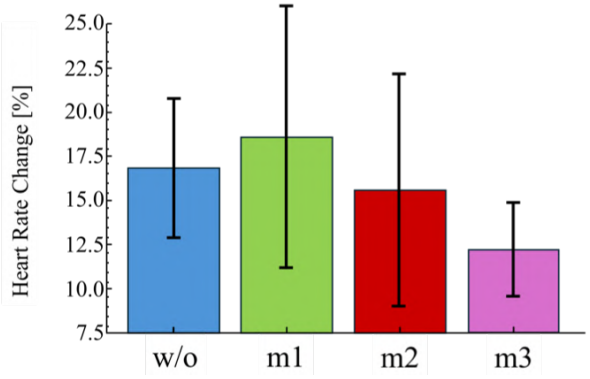

Fig. 15. Average heart rate change before and after 15 minutes walking under across different modes.

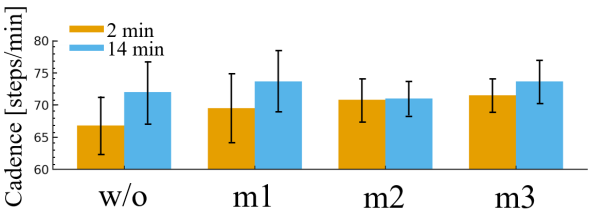

Fig. 16. Mean cadence across modes at 2 and 14 min under user's own comforting walking speed.

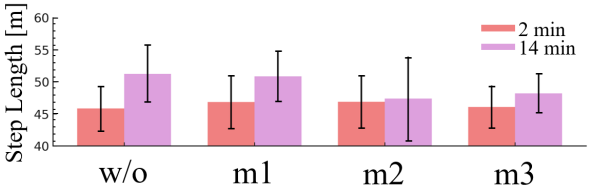

Fig. 17. Mean stride length across modes at 2 and 14 min under user's own comforting walking speed.

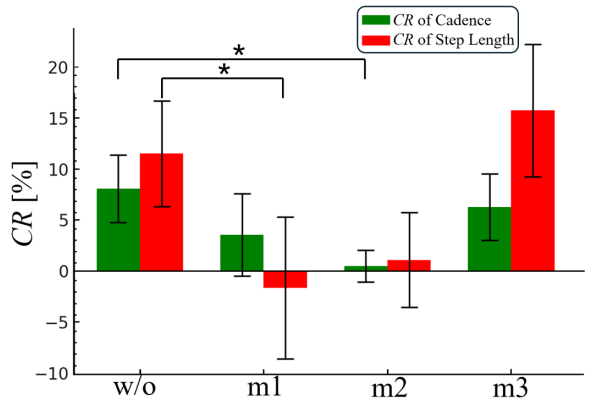

Fig. 18. Ratio comparison of average change rate of cadence and stride length under user's own comforting walking speed.

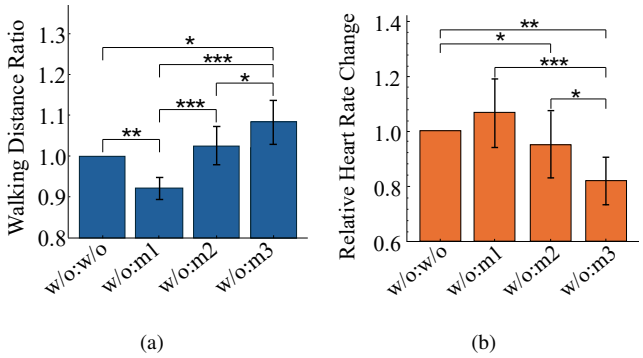

(a) (b)

Fig. 19. Comparing ratio of change rate between modes and without-assustabce. (a) Comparing ratio of walking distance under user's own comforting walking speed. (b) Comparing ratio of heart rate change under user's own comforting walking speed.

pared with the without-assistance condition. In fact, Mode 1 even reduced stride length, suggesting a potential negative effect, while Mode 2 with torque assistance failed to yield substantial benefits. By contrast, Mode 3 demonstrated clear gait enhancement, with increased cadence and decreased stride length, indicating a lighter and more effortless walking pattern.

A direct comparison between Mode 1 and the baseline highlights the limitations of non-phase-aware assistance. Mode 1, which followed fixed speed trajectories from healthy gait templates, paradoxically increased cardiovascular load and reduced walking distance. This outcome can be explained by the device's reliance on preset cycle ratios, which constrain ankle motion during push-off. When users attempted to "kick more" through plantarflexion at the end of Phase 3, the trajectory limits generated resistance, reducing propulsion effectiveness. Furthermore, because participants walked at self-selected speeds, some consciously slowed their cadence to stay synchronized with the device, which further reduced efficiency. These combined factors explain the decreased walking distance and elevated heart rate under Mode 1.

Modes 2 and 3 improved performance by adopting torque control in Phase 3, which reinforced users' voluntary plantarflexion rather than opposing it. Among them, Mode 3 consistently outperformed Mode 2 in walking distance and heart rate reduction. The key distinction lies in Mode 3's free control during Phase 1 and Phase 5, where torque demand is minimal and joint motion changes rapidly. Allowing the ankle to move freely in these phases reduced mechanical interference and improved biomechanical compatibility. This mixed strategy—targeted torque support in propulsion and passive motion in low-demand phases—reduced physiological load, preserved natural rhythm, and enhanced gait comfort.

These results indicate that Mode 3 achieves the best balance of assistance and user adaptability, offering a promising foundation for future clinical applications.

VI. Conclusion

This study developed and validated an ankle-assist system that adapts motor output to gait phases through sensor fusion and mixed control. By integrating IMU and plantar pressure data with phase-specific switching among speed, torque, and free modes, the system achieved accurate phase recognition and targeted motor support. Experiments demonstrated that mixed control outperformed single-mode strategies, improving cadence, stride length, and walking distance while reducing cardiovascular load and maintaining user comfort. These results confirm the effectiveness of adaptive, phase-specific assistance in enhancing gait efficiency and reducing effort. However, the currennt system is only limited to a certain walking speed, and validated on young healthy males. It is expected to be validated on elderly and impaired populations in the future. Looking ahead, the system can be extended to user-specific gait patterns, speeds, and terrains, with advanced learning methods further refining phase recognition and adaptive control. With large-scale validation, this approach has strong potential for rehabilitation and daily mobility support in elderly and impaired populations.

Appendix

Video of the results can be seen on the following link: `https://youtu.be/93YIq_J7qe8`

Acknowledgments

We would like to thank all participants for their cooperation, in which the experiment involving human participants is under the approval (2024-595) of the Ethics Review Committee of Waseda University.

References

[1] Y. Tanimoto, M. Watanabe, R. Kono, C. Hirota, K. Takasaki, and K. Kono, "Aging changes in muscle mass of japanese," *Japanese Journal of Geriatrics*, vol. 47, no. 1, pp. 52–57, 2010.

[2] F. Sakr, J. Safwan, M. Cherfane, P. Salameh, H. Sacre, C. Haddad, S. El Khatib, M. Rahal, M. Dia, A. Harb, H. Hosseini, and K. Iskandar, "Knowledge and awareness of stroke among the elderly population: Analysis of data from a sample of older adults in a developing country," *Medicina*, vol. 59, no. 12, p. 2172, 2023.

[3] C.-D. Lee, A. R. Folsom, and S. N. Blair, "Physical activity and stroke risk: A meta-analysis," *Stroke*, vol. 34, no. 10, pp. 2475–2481, 2003.

[4] S. Gallanagh, T. J. Quinn, J. Alexander, and M. R. Walters, "Physical activity in the prevention and treatment of stroke," *ISRN Neurology*, vol. 2011, p. 953818, 2011.

[5] E. Tanaka, J. R. Zhuang, H.-H. Lee, and L. Yuge, "A walking promotion method using the tuning of a beat sound based on a two-dimensional emotion map," in *Proceedings of International Conference on Human–Computer Interaction (HCI International)*, 2016, pp. 519–525.

[6] J. R. Zhuang, Y. J. Guan, H. Nagayoshi, L. Yuge, H.-H. Lee, and E. Tanaka, "Two-dimensional emotion evaluation with multiple physiological signals," in *Advances in Affective and Pleasurable Design: Proceedings of the AHFE 2018 International Conference on Affective and Pleasurable Design*, 2019, pp. 158–168.

[7] J. R. Zhuang, H.-H. Lee, L. Yuge, and E. Tanaka, "Applying the interaction of walking-emotion to an assistive device for rehabilitation and exercise," in *Proceedings of IEEE/RSJ International Conference on Intelligent Robots and Systems (IROS)*, 2019, pp. 6489–6494.

[8] Y. Li, Z. Gao, I. Kim, and E. Tanaka, "Development of automatic controlled walking assistive device based on fatigue and emotion detection," *Journal of Robotics and Mechatronics*, vol. 34, no. 6, pp. 1383–1397, 2022.

[9] H. Kawamoto, S. Lee, S. Kanbe, and Y. Sankai, "Power assist method for hal-3 using emg-based feedback controller," in *SMC'03 Conference Proceedings. 2003 IEEE International Conference on Systems, Man and Cybernetics. Conference Theme - System Security and Assurance (Cat. No.03CH37483)*. IEEE, 2003, pp. 1648–1653.

[10] A. Esquenazi, M. Talaty, A. Packel, and M. Saulino, "The rewalk powered exoskeleton to restore ambulatory function to individuals with thoracic-level motor-complete spinal cord injury," *American Journal of Physical Medicine and Rehabilitation*, vol. 91, pp. 911–921, 11 2012.

[11] H. Yusa, E. Tanaka, and L. Yuge, "Development of a walking assistance apparatus using a spatial parallel link mechanism and evaluation of muscle activity," in *Proceedings of IEEE International Symposium on Robot and Human Interactive Communication (RO-MAN)*, 2010, pp. 151–158.

[12] E. Tanaka, T. Suzuki, S. Saegusa, and L. Yuge, "Walking assistance apparatus able to select the control method according to the purpose of the user," in *Proceedings of World Automation Congress (WAC)*, 2014, pp. 537–542.

[13] B.-R. Yang, H.-H. Lee, and E. Tanaka, "Posture compensation of a walking assistive device using zero-moment point to stabilize motions on stairs," *Journal of Advanced Mechanical Design, Systems, and Manufacturing*, vol. 14, no. 3, p. A36, 2020.

[14] S.-H. Yu, B.-R. Yang, H.-H. Lee, and E. Tanaka, "A ground-stair walking strategy of the assistive device based on the rgb-d camera," in *Proceedings of IEEE International Conference on Consumer Electronics – Taiwan (ICCE-TW)*, 2021, pp. 341–346.

[15] Y. Fang, Y. Fan, Z. Li, S. Wu, X. Chen, H. Wang, and Q. Zhou, "A stepper motor-powered lower limb exoskeleton with multiple assistance functions for daily use by the elderly," *Journal of Robotics and Mechatronics*, vol. 35, no. 3, pp. 601–611, 2023.

[16] E. Tanaka, R. Niwa, K. Osawa, K. Watanuki, and L. Yuge, "Motion assistance apparatus enabled for neuro-rehabilitation of patients and for the promotion of exercise for the elderly," in *Proceedings of IEEE/ASME International Conference on Advanced Intelligent Mechatronics (AIM)*, 2015, pp. 937–942.

[17] E. Tanaka, K. Muramatsu, K. Watanuki, and L. Yuge, "Development of a walking assistance apparatus for gait training and promotion of exercise," in *Proceedings of IEEE International Conference on Robotics and Automation (ICRA)*, 2016, pp. 3711–3716.

[18] T. Ikehara, K. Nagamura, T. Ushida, E. Tanaka, S. Saegusa, S. Kojima, and L. Yuge, "Development of closed-fitting-type walking assistance device for legs and evaluation of muscle activity," in *Proceedings of IEEE International Conference on Rehabilitation Robotics (ICORR)*, 2011.

[19] J. Li, K. Yang, and D. Yang, "Wearable ankle assistance robot for a human walking with different loads," *Mechanical Sciences*, vol. 14, pp. 429–438, 2023.

[20] L. Yu, H. Leto, and S. Bai, "Design and gait control of an active lower limb exoskeleton for walking assistance," *Machines*, vol. 11, no. 9, p. 864, 2023.

[21] G. Orekhov, Y. Fang, C. F. Cuddeback, and Z. F. Lerner, "Usability and performance validation of an ultra-lightweight and versatile untethered robotic ankle exoskeleton," *Journal of NeuroEngineering and Rehabilitation*, vol. 18, p. 163, 2021.

[22] Y. Bougrinat, S. Achiche, and M. Raison, "Design and development of a lightweight ankle exoskeleton for human walking augmentation," *Mechatronics*, vol. 64, p. 102297, 2019.

[23] B. Chen, C. Shi, C. Zheng, Z. Li, Z. Mei, S. Wang, Y. Li, and X. Wu, "Development of lower limb exoskeleton for walking assistance using energy recycled from human knee joint," *Journal of Mechanisms and Robotics*, vol. 15, no. 5, p. 051007, 2023.

[24] H. Cao, H. Song, Y. Sun, G. Zhang, and X. Li, "A wearable exoskeleton with posture feedback improves abnormal gait in patients with stroke," *Chinese Journal of Tissue Engineering Research*, vol. 29, no. 24, pp. 5127–5133, 2025.

[25] L. Zhang, Z. Wang, and Y. Li, "Mechanism design of cable-driven multifunctional knee osteoarthritis rehabilitation robot," in *2024 IEEE M2VIP*, Oct 2024.

[26] Y. Htet, B. Behera, and F. O. M. Joseph, "Lower extremity exoskeletons: A systematic review on design, control, and sensing," *Engineering Research Express*, vol. 7, no. 2, 2025.

[27] J. Annisa, M. F. Rahmat, and N. Wahab, "Optimizing pid-based controller utilizing hybrid evolutionary algorithm in electric motor-driven exoskeletons for therapeutic locomotion of stroke patients," in *Proceedings of IEEE ICSIMA*, 2024.

[28] Space Bio-Laboratories Co., Ltd., "Re-gait®," https://spacebio-lab.com/regait/, 2025, accessed Jun. 5, 2025.

[29] H. Wang, D. Wang, S. Yan, C.-W. Wang, K. Osawa, and E. Tanaka, "Development of a mixed-control ankle robot with experimental validation of human walking performance," in *2025 25th International Conference on Control, Automation and Systems*, 2025, pp. 1109–1114.

[30] J. Zhang, P. Fiers, K. A. Witte, R. W. Jackson, K. L. Poggensee, C. G. Atkeson, and S. H. Collins, "Human-in-the-loop optimization of exoskeleton assistance during walking," *Science*, vol. 356, no. 6344, pp. 1280–1284, 2017. [Online]. Available: https://www.science.org/doi/10.1126/science.aal5054

[31] Kondo Kagaku, "PMX-SCR-9203HV servo motor," https://kondo-robot.com/product/03217, 2024, product code: 03217. High-torque servo motor, PMX-9200 series, RS-485, 16-bit magnetic encoder.

[32] Arduino, "Arduino Mega 2560 Rev3," https://store-usa.arduino.cc/products/arduino-mega-2560-rev3, 2024, microcontroller board based on ATmega2560; 54 digital I/O, 16 analog inputs, 4 UARTs, 256 KB flash. SKU A000067.

[33] M.-Y. Xu, Y.-F. Hua, Y.-F. Li, J.-R. Zhuang, K. Osawa, K. Nakagawa, H.-H. Lee, L. Yuge, and E. Tanaka, "Development of an ankle assistive robot with instantly gait-adaptive method," *Journal of Robotics and Mechatronics*, vol. 35, no. 3, pp. 669–683, 2023.

[34] InvenSense, a TDK Group Company, "MPU-9250 product specification," https://invensense.tdk.com/wp-content/uploads/2015/02/PS-MPU-9250A-01-v1.1.pdf, 2015, revision 1.1. 9-axis IMU: accelerometer, gyroscope, magnetometer.

[35] J. Kennedy and R. Eberhart, "Particle swarm optimization," in *Proceedings of IEEE International Conference on Neural Networks*, vol. 4, 1995, pp. 1942–1948.

[36] D. Brown, W. Christian, and R. Hanson, "Tracker video analysis and modeling tool," https://physlets.org/tracker/, August 2025, version 6.3.2, Computer software.

[37] Kinovea, "Features of kinovea," https://www.kinovea.org/features.html, 2025, accessed Jun. 9, 2025.

[38] Apple Inc., "View heart rate data on apple watch," https://support.apple.com/en-us/111918, 2025, accessed Jun. 5, 2025.

[39] M. Friedman, "The use of ranks to avoid the assumption of normality implicit in the analysis of variance," *Journal of the American Statistical Association*, vol. 32, no. 200, pp. 675–701, 1937.

[40] F. Wilcoxon, "Individual comparisons by ranking methods," *Biometrics Bulletin*, vol. 1, no. 6, pp. 80–83, 1945.